Experimental and Computational Study on a Variety of Structural Motifs and Coordination Modes in Aluminium Complexes of Di(2-pyridyl)amides and -phosphanides

Matthias Pfeiffer,[a] Alexander Murso,[a] Lepakshaiah Mahalakshmi,[a] Damien Moigno,[b] Wolfgang Kiefer,[b] and Dietmar Stalke*[a]

Keywords: Aluminium / Computational chemistry / Conformation analysis / N ligands / P ligands

The $(2\text{-Py})_2N^-$ ligand shows much more conformational freedom than the $(2\text{-Py})_2P^-$ anion in aluminium coordination. The two isomers $[Al\{(NPy)Py\}_3]$ (**1a**) and $[Al\{(NPy)Py\}_2(Py_2N)]$ (**1b**) were isolated, the former containing exclusively *cis-trans* ligands, and the latter *cis-trans* ligands together with a *trans-trans* ligand. The energy differences in the noncoordinated anions $(2\text{-Py})_2E^-$ (E = N, P) were determined by computational methods to be low in the amide. While the N→Al donor bond energy is appreciable (96 kJ/mol), that of the P→Al donor bond is much lower (45 kJ/mol). This explains why the P-analogous donor-acceptor complex to $Et_2Al(2\text{-Py})_2N{\rightarrow}AlEt_3$ could never be isolated. The P-centred systems are much better π-donors to soft metals than σ-donors to hard metals.

Introduction

Since the historic discovery of Ziegler−Natta catalysts for polymerisation reactions, the industrial importance of organoaluminium compounds has expanded into several other fields, including applications as ceramic precursors, as volatile organometallic precursors for semiconducting materials in electronic industry, and as selective reagents in organic synthesis.[1] Furthermore, current knowledge of the important role of cationic group-13 complexes in catalytic chemistry has resulted in a resurgence of interest in the field of catalytic chemistry.[2] On the other hand, interest in aluminium amide chemistry is due to the potential for the preparation of aluminium nitride thin films.[3] The aluminium nitride can adopt a great variety of structural motifs, oligomerisation through the bridging amido nitrogen atom normally being observed.[4] Suitable tuning of steric factors, however, can prevent such oligomerisation, resulting in monomeric aluminium complexes, as reported by several research groups[5] ($[Al\{N(SiMe_3)_2\}_3]$[5a] and $[AlH_2\{N\text{-}CMe_2CH_2)_2CH_2\}(NMe_3)]$[5b]). Heteroaromatic substituted amides capable of intramolecular side arm donation were found to be able to give rise to several different coordination modes.[6] The presence of diverse donor groups integrated in the ligand periphery can provide electronic and steric stabilisation to the aluminium atom.[5c,5d] During our study on the reactivity and coordination behaviour of 2-pyridyl-based ligand systems[6] − 2-pyridyl derivatives of methane,[7] amines,[8,9] phosphanes,[9,10] arsanes,[10b] phosphanylamines,[11,12a] iminophosphoranes[11,12] and amino-iminophosphoranes[11] − we have isolated several aluminium complexes. The structural variety and large number of coordination modes possible in the case of pyridylamide-based systems[8,9,13] prompted us to carry out a detailed structure and bonding study of dipyridylamide-based aluminium complexes. This paper deals with both crystallographic and theoretical investigations into the structures of some of the aluminium complexes isolated in this group.

Results and Discussion

Syntheses and Crystal Structure of $[Al\{(NPy)Py\}_3]$ (1a) and $[Al\{(NPy)\ Py\}_2\ (Py_2N)]$ (1b)

$LiAlH_4$ is extensively used as a reagent in organic chemistry.[14a,14b] Nöth et al. described the reaction of secondary aliphatic amines with $LiAlH_4$,[14c] we reported the isolation of the intermediate product obtained in the reaction between $(Me_3Si)_2NH$ and $LiAlH_4$ in 1992,[14d] and analogous reactions between $LiAlH_4$ and primary and secondary aromatic amines were reported by Roesky et al. in 1997.[14e] In continuation of our research into the reactivity of $LiAlH_4$ we investigated its reaction behaviour with $(2\text{-Py})_2NH$.

In a reaction similar to that reported by Raston et al.,[13e] treatment of $(2\text{-Py})_2NH$ with $LiAlH_4$ in Et_2O, replacement

[a] Institut für Anorganische Chemie der Universität Würzburg, Am Hubland, 97074 Würzburg, Germany
Fax: (internat.) + 49-(0)931/888-4619
E-mail: dstalke@chemie.uni-wuerzburg.de
[b] Institut für Physikalische Chemie der Universität Würzburg, Am Hubland, 97074 Würzburg, Germany
Supporting information for this article is available on the WWW under http://www.eurjic.org or from the author.

of the solvent by pyridine, subsequent filtration of the undissolved material, and cooling of the solution to 0 °C gives the aluminium triamide [Al{(NPy)Py}$_3$] (**1a**). However, a significantly higher yield of **1a** is obtained on treatment of (2-Py)$_2$NH with Et$_3$Al in Et$_2$O at −78 °C. Stirring for 2 d at room temperature and storage of the resulting solution at −40 °C give crystals of **1a** in 90% yield (Scheme 1). Raston et al.[13e] observed dynamic behaviour of **1a** in solution, as a consequence of which they were unable to distinguish the coordinated and uncoordinated nitrogen atoms of the pyridyl rings in NMR experiments. This dynamic behaviour can be explained by the rearrangement process associated with the ligands, confirmed by the isolation of the isomer **1b** in our studies. In this work, however, eight signals in the ^{1}H NMR and ten signals in the ^{13}C NMR could, as expected, be detected in the solid state structure for the coordinated and the uncoordinated pyridyl rings.

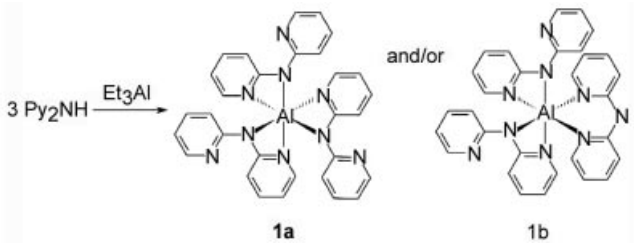

Scheme 1. Synthesis of [Al{(NPy)Py}$_3$] (**1a**) and [Al{(NPy)Py}$_2$-(Py$_2$N)] (**1b**)

Figure 1 shows the molecular structure of **1a**. The geometric features correspond to data obtained from crystals grown after the reaction between (2-Py)$_2$NH and LiAlH$_4$. Three uncoordinated pyridine molecules are present in the asymmetric unit of **1a**. The aluminium amide was isolated several times under different reaction conditions and from various solvents, with the same structural data being obtained in each case. The details show that **1a** incorporates various lattice solvents in different amounts, either as [Al{(NPy)Py}$_3$] + 3PyH (**1a**), [Al{(NPy)Py}$_3$] + thf (space group $P\bar{1}$) or solvent-free [Al{(NPy)Py}$_3$] (space group $P2_1/n$).

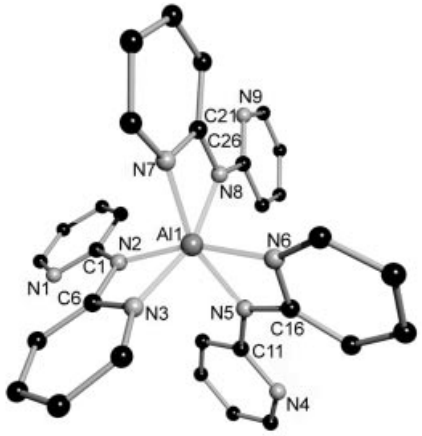

Figure 1. Structure of [Al{(NPy)Py}$_3$] (**1a**) in the solid state; the three pyridine molecules in the lattice have been omitted for clarity

In the solid state, **1a** is a monomer. Each of the three Py$_2$N$^-$ ligands in **1a** adopts a *cis-trans* conformation and exhibits a chelating coordination mode to the aluminium atom. Each Py$_2$N$^-$ ligand coordinates to the metal atom through one pyridyl nitrogen atom and the bridging nitrogen atom of the ligand. The geometry around the aluminium atom is distorted octahedral [N−Al−N angles 66.7(7)−160.37(7)°; Table 1]. The average bond length of 197.3(2) pm for Al1−N(bridge) is slightly shorter than the average bond length of 200.6(2) pm for Al1−N(pyridyl). Both distances, however, are considerably longer than the amidic Al−N single-bond length of 178 pm found in tricoordinate aluminium amide systems such as [Al{N(SiMe$_3$)$_2$}$_3$],[5a] which is due to the higher coordination number of six found in **1a**. On the other hand, the bond lengths are on average 7 pm shorter than in a purely dative Al←N(PyH) bond, with a length of 206 pm in [(PyH)$_3$AlCl$_3$][5e] or 205.7 pm in [Me$_3$Al(Py$_3$P)].[6,10]

The Py$_2$N$^-$ anion in [Al{(NPy)Py}$_3$] (**1a**) coordinates to the metal atom in a *cis-trans* conformation, as previously found in [Me$_2$Tl{(NPy)Py}]$_n$ (see Scheme 2).[8] The Py$_2$N$^-$ ligand is nearly planar, as the angle between the two pyridyl ring planes is only 9° on average, leaving the bridging nitrogen atom sp^2-hybridised. The aluminium atom is displaced at an average distance of 7.5 pm out of the plane of the coordinating rings. NMR spectroscopic studies show that the structure in solution emulates that in the solid state. The ^{1}H NMR spectrum obtained in C$_6$D$_6$ shows the expected eight signals in the aromatic region, while the ^{13}C NMR spectrum displays ten resonances. Dynamic behaviour was not detected at room temperature.

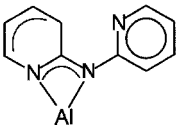

Scheme 2. Mesomeric structure of Py$_2$N$^-$ in [Al{(NPy)Py}$_3$] (**1a**)

Slow evaporation of the deuterated NMR solvent from a sample of **1a** at room temperature resulted in the recrystallisation of a aluminiumtris[di(2-pyridyl)]amide that turned out to be a different conformational isomer [Al{(NPy)Py}$_2$(Py$_2$N)] (**1b**). This isomer contains two C$_6$D$_6$ molecules in the asymmetric unit rather than the three pyridine molecules in **1a**.

In the solid state, **1b** is found to be a monomer similar to **1a**. The three Py$_2$N$^-$ ligands chelate the aluminium atom and the metal centre exists in a distorted octahedrally coordinated polyhedron [N−Al−N angles vary from 64.69(17) to 167.8(2)°]. However, one of the Py$_2$N$^-$ ligands in [Al{(NPy)Py}$_2$(Py$_2$N)] (**1b**) now adopts a *trans-trans* conformation and coordinates to the aluminium atom through both pyridyl nitrogen atoms, leaving one bridging nitrogen atom uncoordinated (Figure 2, Table 2). The bond parameters of the *cis-trans* ligand containing N1 to N3 indicate a bonding situation similar to that of the Py$_2$N$^-$ ligands in **1a**.

Table 1. Selected average bond lengths [pm] and angles [°] in [Al{(NPy)Py}$_3$] (**1a**); the tabulated structural parameters correspond to the average values for the di(2-pyridyl)amide ligand according to the numbering scheme

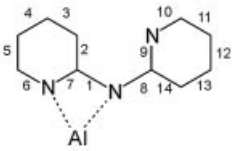

Al1−N(bridge)	197.3(2)	Al1−N(pyridyl)	200.6(2)	1	137.3(2)
2	139.9(3)	3	137.6(3)	4	137.5(3)
5	137.0(3)	6	133.7(2)	7	136.1(2)
8	138.6(3)	9	134.1(2)	10	134.4(2)
11	136.8(2)	12	138.3(3)	13	137.1(2)
14	140.2(3)	N(coord. pyridyl)···N(bridge)	218.6		
N(noncoord. pyridyl)···N(bridge)	236.2				
N2−Al1−N6	158.10(7)	N8−Al1−N3	160.37(7)	N5−Al1−N7	156.81(7)
N2−Al1−N5	103.46(7)	N8−Al1−N2	104.92(7)	N5−Al1−N8	106.24(7)
N(pyridyl)−Al1−N(bridge)	66.7(7)	C(*ipso*)−N(bridge)−C(*ipso*)	124.8(2)		

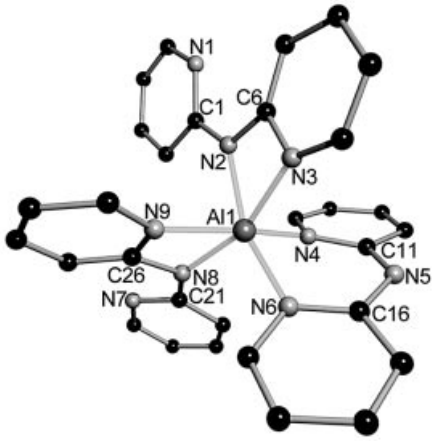

Figure 2. Structure of [Al{(NPy)Py}$_2$(Py$_2$N)] (**1b**) in the solid state; the two C_6D_6 molecules in the lattice have been omitted for clarity

The situation in the second *cis-trans* ligand, between the atoms from N7 to N9, is quite different from that in **1a**. The variance of the two Al−N bonds is larger [Al1−N8 197.0(5) and Al1−N9 202.5(4) pm]. This indicates a greater accumulation of charge density at the bridged nitrogen atom N8, which is further supported by the angle defined by the best planes between the two pyridyl rings. This large angle of 17.7°, in contrast to the average 9° in **1a** and 7.2° in the previous ligand (N1 to N3) in **1b**, points to more pronounced sp^3 hybridisation at the bridging nitrogen atom N8. The aluminium atom is found at a distance of 31.5 pm out of the heteroallyl system plane, in contrast to the analogous distance of just 7.5 pm in **1a**.

Similarly, the *trans-trans* conformation of the Py$_2$N$^-$ ligand in [Al{(NPy)Py}$_2$(Py$_2$N)] (**1b**) shows another structural feature different to that found in [Me$_2$Al(Py$_2$N)] (Scheme 3).[8] Although both ligands show similar coordination to the metal atom, with the N−C bond lengths in [Me$_2$Al(Py$_2$N)] indicating a symmetric charge distribution over both pyridyl rings, they are unsymmetrical in **1b**. This can be seen in all the N(bridge)−C(*ipso*), C(*ipso*)−N(pyridyl) and Al−N bond lengths. Regardless of the fact that both pyridyl rings take part in the metal coordination, the greater part of the electron density is accumulated in only one of them (C11−C15 and N4). This results in shorter Al1−N4 [196.9(4) compared to 200.9(5) pm for Al1−N6] and N5−C11 bonds [134.2(7) in comparison to 139.3(7) pm for N5−C16]. In solution, **1b** converts into the conformational isomer **1a**, and so no difference is observed in the spectroscopic data. Conformer **1b** seems to be energetically disfavoured in comparison to **1a**, but can be crystallised under the conditions described in the Exp. Sect.

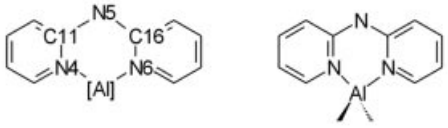

Scheme 3. The *trans-trans* conformation of Py$_2$NH$^-$ in [Al{(NPy)Py}$_2$(Py$_2$N)] (**1b**) and [Me$_2$Al(Py$_2$N)]

Syntheses and Crystal Structure of [(PyH)$_2$AlCl$_2${(NPy)Py}] (2)

A solution of di(2-pyridyl)amine and aluminium trichloride, when treated with *n*-butyllithium and allowed to warm to room temperature, gives [(PyH)$_2$AlCl$_2${(NPy)Py}] (**2**) (Scheme 4). Colourless crystals of **2** were isolated after 4 d at 0 °C. The crystals were found to decompose at 50 °C.

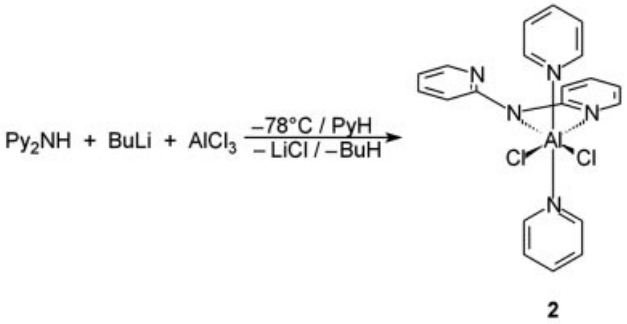

Scheme 4. Synthesis of [(PyH)$_2$AlCl$_2${(NPy)Py}] (**2**)

Table 2. Selected bond lengths [pm] and angles [°] in [Al{(NPy)Py}$_2$(Py$_2$N)] (**1b**)

Al1−N2	201.9(4)	Al1−N3	203.1(5)	Al1−N4	196.9(4)	
Al1−N6	200.9(5)	Al1−N8	197.0(5)	Al1−N9	202.5(4)	
N2−C1	137.4(6)	C1−C2	144.2(8)	C2−C3	140.8(8)	
C3−C4	135.5(9)	C4−C5	132.3(10)	C5−N1	133.8(8)	
N1−C1	135.1(6)	N2−C6	135.4(6)	C6−C7	139.4(7)	
C7−C8	143.6(9)	C8−C9	139.9(8)	C9−C10	133.0(8)	
C10−N3	131.4(7)	N3−−C6	136.5(6)	N5−C11	134.2(7)	
C11−C12	144.3(8)	C12−C13	134.8(8)	C13−C14	137.1(9)	
C14−C15	133.9(9)	C15−N4	133.2(7)	N4−C11	137.3(7)	
N5−C16	139.3(7)	C16−C17	137.5(7)	C17−C18	135.8(8)	
C19−C20	135.8(8)	C20−N6	137.2(6)	N6−C16	135.5(7)	
N8−C21	135.4(7)	C21−C22	139.8(7)	C22−C23	137.1(7)	137.1(7)
C23−C24	136.7(9)	C24−C25	135.2(9)	C25−N7	135.5(8)	
N7−C21	136.1(7)	N8−C26	139.4(7)	C26−C27	137.9(8)	
C27−C28	140.0(8)	C29−C30	138.8(8)	C30−N9	133.8(7)	
N9−C26	133.4(7)					
N2···N3	216.7	N4···N6	276.6	N8···N9	219.6	
N2−Al1−N3	64.69(17)	N4−Al1−N6	88.10(19)	N8−Al1−N9	66.68(19)	
N2−Al1−N6	156.48(19)	N4−Al1−N9	167.8(2)	N8−Al1−N3	160.34(19)	
N2−Al1−N9	88.20(16)	N4−Al1−N2	90.87(17)	N8−Al1−N4	101.7(2)	
C1−N2−C6	124.9(4)	C11−N5−C16	125.1(5)	C21−N8−C26	127.2(5)	

Compound **2** exists as a monomer in the solid state (Figure 3). Di(2-pyridyl)amide coordinates to the aluminium atom through one of the pyridyl ring nitrogen atoms and the bridging central nitrogen atom. The coordination sphere is completed by the coordination of two chloro ligands and the nitrogen atoms of two pyridine molecules to give a distorted octahedral geometry around the aluminium centre (N5−Al1−N4 174.4°, Cl1−Al1−Cl2 137.5°, N2−Al1−N3 65.9°). Because of the absence of steric strain the two pyridyl rings are coplanar.

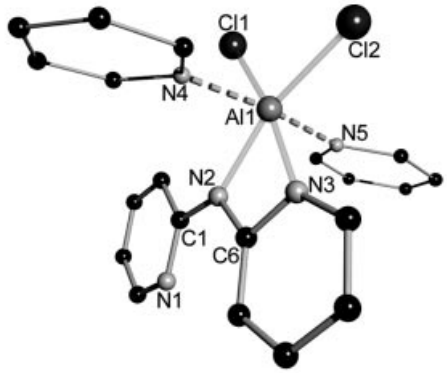

Figure 3. Structure of [(PyH)$_2$AlCl$_2${(NPy)Py}] (**2**) in the solid state

The di(2-pyridyl)amide ligand in **2** adopts a *cis-trans* conformation, as in the cases of **1a** and [Me$_2$Tl{(NPy)Py}]$_n$ [8] (Figure 3, Table 3). The distance between the coordinated central nitrogen atom and the pyridyl nitrogen atom is 218.1 pm. In the octahedral coordination sphere, the aluminium atom lies nearly in the plane of the di(2-pyridyl)amide ligand (7.6° angle between the pyridyl ring planes) in the Al1−Cl1−Cl2 plane. This is the first example of *cis-trans* coordination of the monoanionic di(2-pyridyl)amide in a monomeric metal complex. As in **1a** and **1b**, the *cis−cis* conformation is precluded due to the greater N_{ring}···N_{ring} distance, while in a hypothetical planar *trans-trans* conformation there would be steric interaction between the hydrogen atoms of the ring and the chlorine atoms, due to their closer proximity. Hence, by adopting the *cis-trans* conformation, the system avoids such disadvantageous steric factors (Scheme 5). Because of the coordination through the central nitrogen atom N2 and through the pyridyl nitrogen atom N3 of the di(2-pyridyl)amide, different electronic situations exist in the pyridyl rings. The distances from the bridging nitrogen atom N2 to the *ipso*-carbon atoms (N2−C1 139.3 and N2−C6 136.8 pm) deviate significantly in the same way as seen for the C_{ipso}−N_{ring} distance (C6−N3 136.8 and C1−N1 134.2 pm). The N2−C6 bonding exhibits a more pronounced double bond character, in contrast to N2−C1. Furthermore, C6−N3 is shorter than C1−N1. The charge of the anionic ligand is predominantly localised at the N3 nitrogen atom of the coordinated pyridyl ring (Scheme 6).

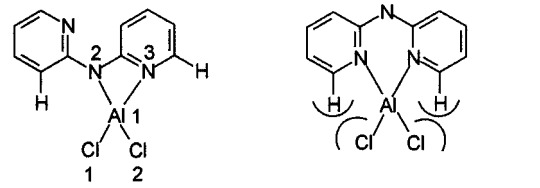

Scheme 5. View of [(PyH)$_2$AlCl$_2${(NPy)Py}] (**2**) along the N_{PyH}−Al−N_{PyH} axis (left) and the precluded *trans-trans* arrangement (right)

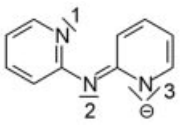

Scheme 6. The mesomeric structures of the di(2-pyridyl)amide ligand in [(PyH)$_2$AlCl$_2${(NPy)Py}] (**2**)

Table 3. Selected bond lengths [pm] and angles [°] in $[(PyH)_2AlCl_2\{(NPy)Py\}]$ (**2**)

Al1−Cl1	223.7(2)	Al1−N3	198.4(3)	Al1−N2	202.7(3)
Al1−Cl2	226.2(1)	Al1−N4	205.9(3)	Al1−N5	207.7(3)
C1−C2	139.9(5)	C2−C3	138.0(5)	C3−C4	137.4(6)
C4−C5	137.0(6)	C5−N1	134.7(5)	N1−C1	134.2(5)
C1−N2	139.3(4)	N2−C6	136.8(5)	C6−C7	139.9(5)
C7−C8	136.6(5)	C8−C9	138.7(6)	C9−C10	135.5(6)
C10−N3	133.8(5)	N3−C6	136.8(4)	N4−C11	135.2(4)
N4−C15	133.9(5)	N5−C16	134.5(5)	N5−C20	134.5(5)
Cl1−Al1−Cl2	137.5(1)	N5−Al1−N4	174.3(1)	N5−Al1−N3	88.8(1)
N2−Al1−N3	65.9(1)	N5−Al1−Cl1	91.5(1)	N4−Al1−N2	87.5(1)
N2−Al1−Cl1	104.6(1)	N5−Al1−Cl2	92.8(1)	N4−Al1−N3	87.9(1)
N2−Al1−Cl2	159.5(1)	N4−Al1−Cl1	91.1(1)	N1−C2−N2	119.4(4)
N3−Al1−Cl1	170.4(1)	N4−Al1−Cl2	92.0(1)	N2−C6−N3	105.8(3)
N3−Al1−Cl2	93.6(1)	N5−Al1−N2	86.9(1)	C2−C1−N2	118.7(4)
				C7−C6−N2	135.4(4)

The aluminium−nitrogen and aluminium−chloride distances in **2** can be compared with those in the following compounds: $[Cl_2Al(PyH)_4][AlCl_4]$ (Al−N 206, Al−Cl 227 pm),[5e] $Cl_3Al(PyH)_3$ (Al−N 206, Al−Cl 227 pm),[5e] and $Cl_2Al(bpy)_2$ (Al−N 203, Al−Cl 225 pm).[5f] The Al1−N4 (205.9 pm) and Al1−N5 (207.7 pm) bond lengths in the donating pyridine molecules correspond to the dative aluminium−nitrogen bonding in $[Cl_2Al(PyH)_4][AlCl_4]$[5e] and $[Cl_3Al(PyH)_3]$,[5f] each with an Al−N distance of 206 pm. The aluminium−nitrogen bonds in the monoanionic di(2-pyridyl)amide ligands are substantially shorter. Because of the higher charge density at the pyridyl ring nitrogen atom N3, the Al1−N3 bond length (198.4 pm) is shorter than the Al1−N2 bond length (202.7 pm).

Both aluminium−chloride bond lengths lie in the range expected for Al−Cl bond lengths (226 pm). However, Al1−Cl1 (223.7 pm) is shorter than Al1−Cl2 (226.2 pm). The different Al−N distances result from the difference in the dipole moment parallel to Al1−N3 and Al1−N2. Thus, the Al−Cl bond length is likewise different. As a compensation for these differences a shortening of the Al1−Cl1 bond and a lengthening of the Al1−Cl2 bond results.

The ^1H and the ^{13}C NMR spectra at room temperature do not resolve the magnetic and chemical differences of the pyridyl substituents. Because of the overlap of the signals in the ^1H NMR spectrum, no exact assignment could be made. Eight signals are observed in the ^{13}C NMR spectrum of **2**; three correspond to the pyridine molecules and four to the di(2-pyridyl)amide ligand [δ = 116.6 (C5), 117.7 (C3), 123.6 (C_{para}), 139.7 (C_{meta}), 141.5 (C4), 142.7 (C_{ortho}), 144.1 (C6), 152.8 (C2) ppm]. NMR experiments conducted at −60°C show no further splitting of the signal pattern.

Comparison of Structural Parameters for Compounds 1a, 1b and 2

Structural comparison of the various complexes shows that the Py_2N^- ligand is flexible enough, depending on the electronic and steric demand, to suit different coordination modes, giving rise to a variety of metal complexes. Scheme 7 illustrates the different possible coordination modes for the dipyridyl amide ligand. Furthermore, the negative charge density at the bridging nitrogen atom of the Py_2N^- ligand is more or less delocalised over the pyridyl ring. The degree of delocalisation and density accumulation depends on the coordinated metal atom, the degree of aggregation and the conformation of the ligand. This has a distinct effect on the geometrical parameters of the ligand, accounting for the significant perturbation of the aromatic ring systems.

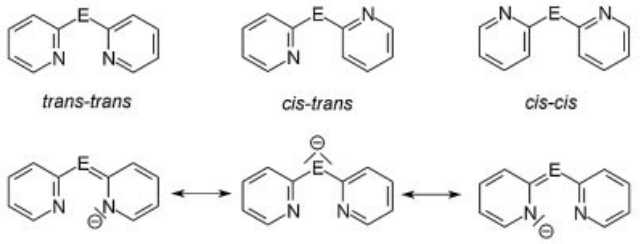

Scheme 7. The different possible coordination modes of the di(2-pyridyl)amide and -phosphanide ligand (top) and the mesomeric structures for the ligand in the *trans-trans* coordination mode (bottom)

Table 4 gives an overview of the structural parameters of the Py_2N^- ligand for compounds **1a**, **1b** and **2**, in comparison with PyH (**A**),[17] $(2\text{-Py})_2NH$ (**B**),[15] $[Me_2Al(Py_2N)]$ (**C**),[8] $[Et_2Al(2\text{-}Py_2N)AlEt_3]$ (**D**),[9] Py_2PH (**E**),[9] $[Me_2Al(Py_2P)]$ (**F**)[10a][10b] and $[Et_2Al(Py_2P)]$ (**G**).[9] The structural parameters shown in Table 4 follow the ordering scheme shown in the Figure. Three different kinds of polymorphs are known for the $(2\text{-Py})_2NH$ molecule; a hydrogen-bridging dimer exists in the orthorhombic[18a] and triclinic[18b] polymorphs, while on the other hand, the hydrogen bridging produces a tetramer in the case of the monoclinic[9] polymorph. Distinct and strong differences exist in the torsion angles (the angle β between the pyridyl planes) of the various polymorphs found in $(2\text{-Py})_2NH$. The angles are 73, 40 and 0° in the triclinic, orthorhombic and monoclinic forms, respectively. However, the bond lengths in the different polymorphs are identical. The free electron pair in neutral $(2\text{-Py})_2NH$ is also partly delocalised over the pyridyl ring. The bridging nitrogen atom has sp^2 character. Assessment of the electronic structure in di(2-pyridyl)amide li-

Table 4. Comparison of the structural parameters of the di(2-pyridyl)amide ligands in compounds **1a**, **1b** and **2** with PyH **(A)**,[17] Py_2NH **(B)**,[15] [$Me_2Al(Py_2N)$] **(C)**,[8] [$Et_2Al(2\text{-}Py_2N)AlEt_3$] **(D)**,[9] Py_2PH **(E)**,[9] [$Me_2Al(Py_2P)$] **(F)**[10a,10b] and [$Et_2Al(Py_2P)$] **(G)**[9]

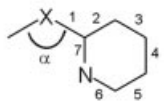

α = C(*ipso*)–N(bridge)–C(*ipso*)
β = angle between the two pyridyl ring planes
X = N, P

[a]	Aggr.	Conf.	1	2	3	4	5	6	7	α	β
A				139.4	139.2	139.2	139.4	133.8	133.8		
B	dimer, tetramer	*cis-trans*	138.0	139.5	137.0	137.0	136.5	134.0	133.5	131.1	
C	monomer	*trans-trans*	134.3	142.1	135.3	139.5	135.5	136.6	136.6	125.5	10.4
D	monomer	*trans-trans*	138.8	139.5	136.2	139.5	135.2	136.7	138.6	122.4	10.4
E		*cis-trans*	186.6	141.1	140.0	140.3	140.3	134.8	135.1	102.6	
F	monomer	*trans-trans*	178.4	141.5	136.2	139.8	135.8	136.2	136.8	106.6	25.0
G	monomer	*trans-trans*	177.8	142.0	135.8	139.0	135.5	136.6	136.8	107.4	17.0
1a	monomer	*cis (c)-*	137.2	139.9	137.6	137.5	137.0	133.7	136.1	124.8	9.0
		trans (nc)	138.6	140.2	137.1	138.3	136.8	134.4	134.1		
1b	monomer	*cis (c)-*	137.2	138.8	140.9	138.7	136.3	132.9	135.1		21.3
		trans (nc)	136.9	141.7	138.8	136.5	134.4	134.7	135.5	125.2	7/18.6
		trans (c)	136.4	141.3	135.4	139.2	135.0	135.6	136.2	125.9	
2	monomer	*cis (c)-*	136.8	139.9	136.6	138.7	135.5	133.8	136.8	123.8	8.2
		trans (nc)	139.3	139.9	138.0	137.4	137.0	134.7	134.2		

[a] The bond lengths correspond to average values for compounds with more than one equivalent pyridyl ring; (c) = coordinated pyridyl ring; (nc) = non-coordinated pyridyl ring; for compound **E** the data correspond to the optimised geometry obtained from DFT calculations with BPW91/6-31+G*, standard bond lengths[16]: N−C 147 pm, N=C 129 pm, C−C 154 pm, C=C 134 pm, P−C 185 pm, P=C 161 pm,[22] N−C 147 pm, N=C 129 pm, C−C 154 pm, C=C 134 pm.

gands in various metal complexes is possible by comparison with $(2\text{-}Py)_2NH$.

Theoretical Studies of the $(2\text{-}Py)_2P^-$ and $(2\text{-}Py)_2N^-$ Anions

To obtain deeper insights [e.g., the energetic differences between the conformers and the quantification of an Al−N(amide) versus Al←N(donor) bond energy contribution in the light of the related $(2\text{-}Py)_2P^-$ phosphanide system] into these structures, we performed DFT calculations. Coordination modes with the *cis-cis*, *cis-trans* and *trans-trans* conformers are documented for both $(2\text{-}Py)_2E^-$ anions (E = N, P).[7,10] Although the bridging nitrogen atom in $Et_2Al(2\text{-}Py)_2N$ might be employed in an additional N→Al donor bond towards $AlEt_3$ to give the adduct $Et_3Al{\leftarrow}N(2\text{-}Py)AlEt_2$, Lewis acid/base pairing was precluded with the related phosphanide $Et_2Al(2\text{-}Py)_2P$.[9] However, the di(2-pyridyl)phosphanide ligand shows a metal-dependent coordination response and is involved in a highly unusual σ/π interaction with the soft metal caesium.[10c] The phosphorus atom in the anion is sufficiently Lewis basic to bridge two soft organometallic iron centres. In this context, the different conformers of $(2\text{-}Py)_2N^-$ and $(2\text{-}Py)_2P^-$ were analysed by DFT calculations (Figure 4).

As anticipated, the *cis-trans* conformers of both $(2\text{-}Py)_2E^-$ anions are more stable than the *trans-trans* and *cis-cis* conformers. The twisted *trans-trans* conformer of Py_2N^- is only 1.4 kJ/mol more stable than the twisted *cis-cis* form (each av. dihedral angle 52°), while the twisted *cis-cis* form of the Py_2P^- anion (each av. dihedral angle 42°) is significantly more stable than the twisted *trans-trans* form (11.42 kJ/mol, Figure 4). This allows full conjugation throughout the heteroallylic system and intramolecular $N^{\delta-}\cdots{}^{\delta+}H(C)$ hydrogen bonding. While the N(bridge)−C(*ipso*) distances from the calculated anions match those in the experimental contact ion pairs **1a**, **1b** and **2** almost exactly, the P(bridge)−C(*ipso*) distances seem to be marginally too long (compare Tables 1−3 and 5). While the C−E−C angle in the amides is widened to values considerably larger than 120°, it is much sharper in the phosphanides, and smaller even than the value expected for an sp^3-hybridised phosphorus atom. Both features match the experimentally found values in the contact ion pairs. Closer examination of the bond lengths reveals partially localised double bonds in the pyridyl rings at the 3- and 5-positions. The small energetic differences between the *trans-trans* and the *cis-trans* conformers − 7.4 kJ/mol for the Py_2N^- and 23.2 kJ/mol for the Py_2P^- anion − can easily be overcompensated by metal coordination.

Theoretical Studies of the E→Al Donor Bond (E = N, P)

The next challenge was to determine the E→Al donor-acceptor bond energies in the experimentally verified complex $Et_2Al(2\text{-}Py)_2NAlEt_3$ and the model compounds $Me_2Al(2\text{-}Py)_2N{\rightarrow}AlMe_3$ and $Me_2Al(2\text{-}Py)_2P{\rightarrow}AlMe_3$, since $Et_2Al(2\text{-}Py)_2P$ does not form the adduct $Et_2Al(2\text{-}Py)_2P{\rightarrow}AlEt_3$ with a second equivalent of $AlEt_3$. One difference between the Lewis-type donor-acceptor bond and a covalent bond is that dissociation of the former yields two

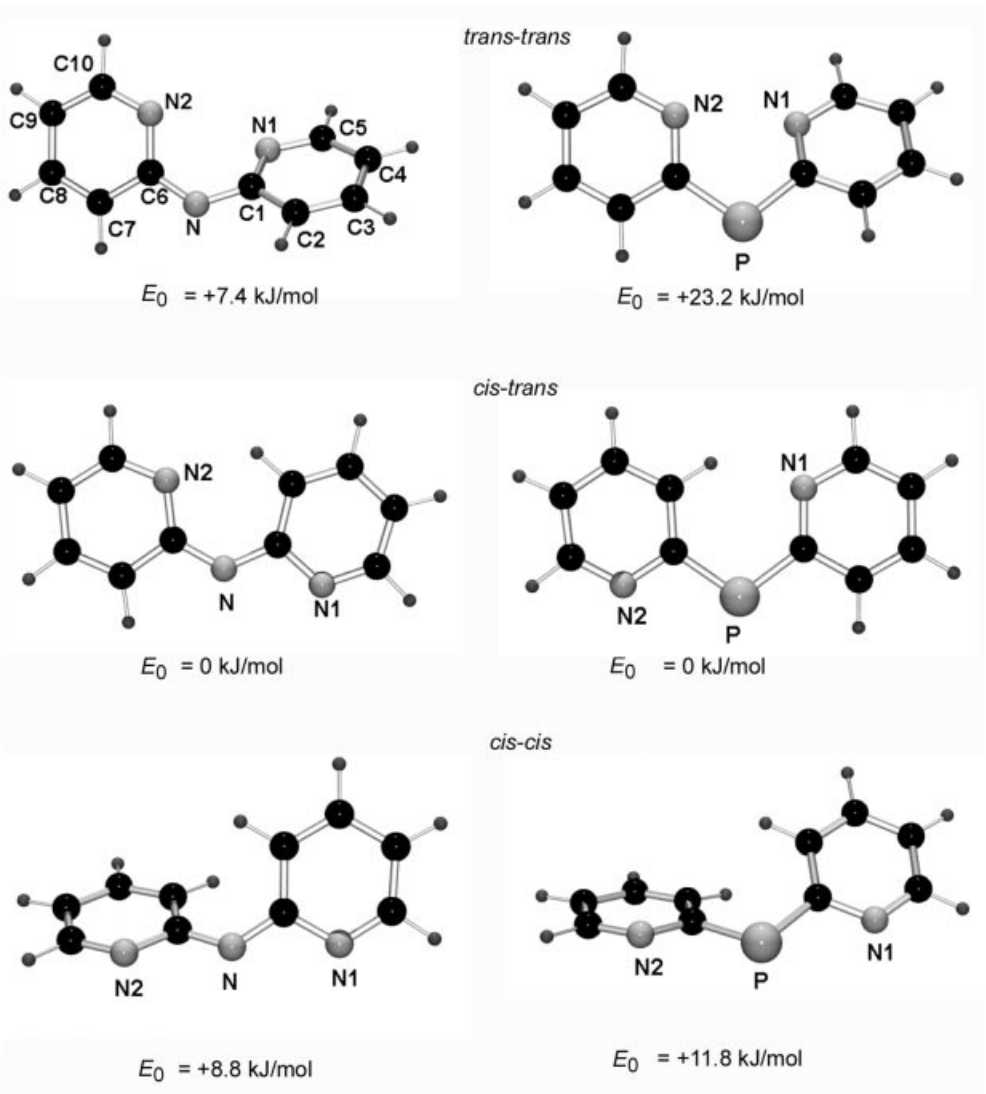

Figure 4. Optimised geometries for the different conformers of the free $(2\text{-Py})_2N^-$ and $(2\text{-Py})_2P^-$ anions by the BPW91/6-31+G(d) method

Table 5. Selected calculated bond lengths [pm] and angles [°] for the free $(2\text{-Py})_2N^-$ and $(2\text{-Py})_2P^-$ anions at the BPW91/6-31+G(d) level of theory

	$(2\text{-Py})_2N^-$			$(2\text{-Py})_2P^-$		
	trans-trans	*cis-trans*	*cis-cis*	*trans-trans*	*cis-trans*	*cis-cis*
E−C1	135.4	136.2	135.1	182.1	182.0	182.2
C1−C2	144.2	144.3	144.6	143.5	143.1	143.4
C2−C3	138.9	139.4	139.0	139.2	139.5	139.2
C3−C4	141.4	140.9	141.3	141.3	141.1	141.2
C4−C5	140.6	140.7	140.6	140.6	140.7	140.6
C5−N1	134.1	133.8	134.0	134.2	134.0	134.1
N1−C1	138.1	138.7	138.5	137.2	138.0	138.2
N1···N2	301.6			308.2		
E−C6	135.4	135.3	135.1	182.1	181.8	182.2
C6−C7	144.2	144.7	144.6	143.5	144.0	143.4
C7−C8	138.9	138.6	139.0	139.2	138.8	139.2
C8−C9	141.4	141.8	141.3	141.3	141.8	141.2
C9−C10	140.6	140.1	140.6	140.6	140.1	140.6
C10−N2	134.1	134.5	134.0	134.2	134.6	134.1
N2−C6	138.1	138.8	138.5	137.2	137.9	138.2
C1−E−C6	124.5	126.5	123.9	107.0	108.4	105.0

closed-shell fragments with an electron lone-pair donor and an electron-pair acceptor, while the latter gives two open-shell fragments.[19] Another difference is that the bond length of a covalent bond would not usually change much in different aggregation states, while donor-acceptor bonds frequently show larger interatomic distances in the gas phase than in the solid state. As we wanted to investigate the above-mentioned donor-acceptor complexes by theoretical methods, we first tested them by employing the molecular structures of the complexes $Me_3N{\rightarrow}AlMe_3$ and $Me_3P{\rightarrow}AlMe_3$, which have already been determined structurally in the gas phase.[20] Their donor-acceptor bond dissociation energies were determined experimentally. The theoretical parameters calculated at the CBS-4, MP2/6-31+G(d) and BPW91/6-31+G(d) levels of theory were evaluated and compared to the experimental values obtained by Haaland. As expected, the most powerful computational methods CBS-4M and MP2/6-31+G(d) gave the best match with the experimentally ascertained structures and energies. The BPW91/6-31+G(d) method calculates the N→Al and P→Al donor-acceptor bond lengths as being

slightly too long, and the resulting bond dissociation energies are too low (Figure 5).

To force the central donating atom into the sp^2 hybridisation of an amide or phosphanide we performed calculations for $H_2C{=}(Me)N{\rightarrow}AlMe_3$ and $H_2C{=}(Me)P{\rightarrow}AlMe_3$, since these models should be more consistent with $Me_2Al(2\text{-}Py)_2N{\rightarrow}AlMe_3$ and $Me_2Al(2\text{-}Py)_2P{\rightarrow}AlMe_3$. In contrast to the shortening of the Al−N bond, by 1 and 5 pm, the P−Al interatomic distances surprisingly lengthened by 5 and 10 pm by the MP2 and BPW91/6-31+G(d) methods, respectively. Furthermore, the calculated bond dissociation energies at the most reliable MP2 level of theory were determined in these cases to be 95.7 and 44.9 kJ/mol for $H_2C{=}(Me)N{\rightarrow}AlMe_3$ and $H_2C{=}(Me)P{\rightarrow}AlMe_3$, respectively (Figure 5). Consequently, the sp^2 hybridisation of the heteroatom and the coupling of the charge to the substituents has a strong effect on the dissociation enthalpy of the E→Al bond, and particularly in the phosphanide adduct. While the energy is only decreased by a factor of one fifth in the amide adduct, it is halved in the phosphanide adduct. In addition, the "hard" aluminium atom prefers the "hard" nitrogen donor rather than the "soft" phosphane function. Population analysis schemes, such as Natural Population Analysis,[21] assign most pronounced negative partial charges to the ring nitrogen atoms in $Me_2Al(2\text{-}Py)_2N$ and $Me_2Al(2\text{-}Py)_2P$. In the latter, the divalent P^{III} centre even shows a partial positive charge. (Scheme 8).

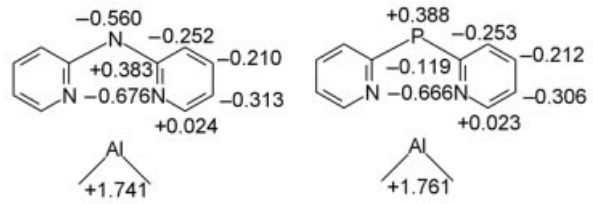

Scheme 8. Calculated natural charges in $[e]^-$ for the complexes $Me_2Al(2\text{-}Py)_2N$ and $Me_2Al(2\text{-}Py)_2P$, determined by natural population analysis

The s and p_π populations of the atomic orbitals of the bridging phosphorus and nitrogen atoms are significantly different. The 3s orbital in the phosphorus atom is more highly populated than the 2s orbital of the nitrogen atom, while the charge density in the p orbitals of the phosphorus atom is depleted relative to the bridging nitrogen atom.

Since this suggests the formation of a metal−nitrogen bond rather than a metal−phosphorus bond, we became interested in quantitatively evaluating the E→Al bond energies in the model compounds $Me_2Al(2\text{-}Py)_2N{\rightarrow}AlMe_3$ and $Me_2Al(2\text{-}Py)_2P{\rightarrow}AlMe_3$. Selected bond lengths and angles for these compounds are reported in Table 6, in comparison

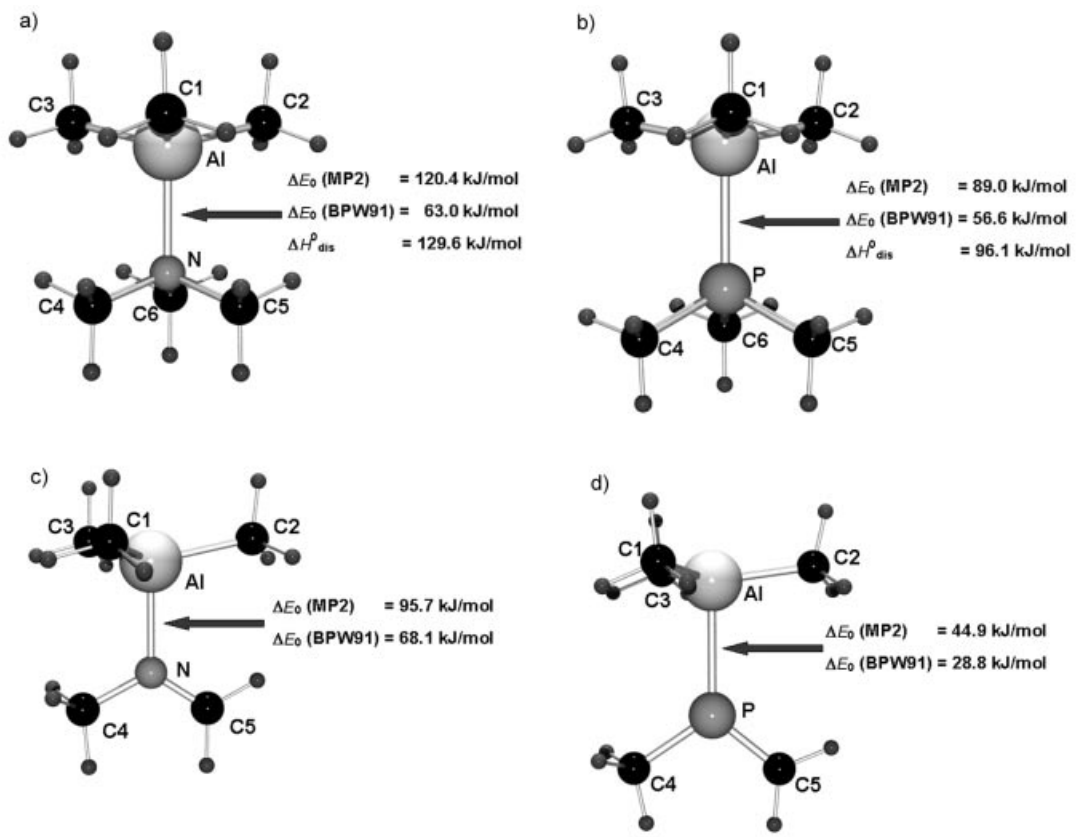

Figure 5. Optimised geometries for the adducts $Me_3N{\rightarrow}AlMe_3$ (a), $Me_3P{\rightarrow}AlMe_3$ (b), $H_2C{=}(Me)N{\rightarrow}AlMe_3$ (c) and $H_2C{=}(Me)P{\rightarrow}AlMe_3$ (d), with the related E→Al donor bond energies

Table 6. Selected calculated bond lengths [pm] and angles [°] of $Me_2Al(2\text{-}Py)_2N{\rightarrow}AlMe_3$ and $Me_2Al(2\text{-}Py)_2P{\rightarrow}AlMe_3$ in comparison to the experimentally ascertained data for $Et_2Al(2\text{-}Py)_2N{\rightarrow}AlEt_3$

E = N

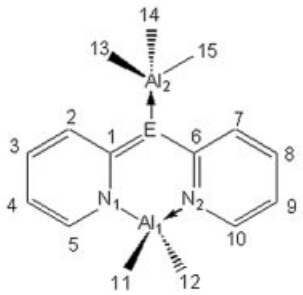

E = P

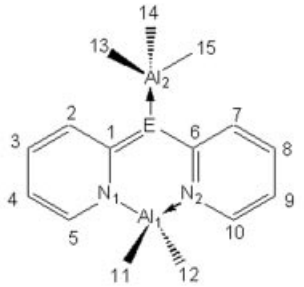

	BPW91/6-31+G(d)	Expt.	BPW91/6-31+G(d)
E−C1/E−C6	137.8	138.3(4)/139.2(5)	180.4
E−Al2	212.9	201.0(3)	266.0
C1−C2/C6−C7	142.5	137.2(6)/140.7(5)	143.0
C2−C3/C7−C8	138.6	137.0(5)/135.5(5)	138.6
C3−C4/C8−C9	141.3	139.5(5)	141.7
C4−C5/C9−C10	138.4	134.0(5)/136.7(5)	138.5
C5−N1/C10−N2	136.7	138.0(5)/135.4(4)	136.8
N1−C1/N2−C6	137.7	138.0(5)/136.2(5)	138.5
N1−Al1/N2−Al1	197.8	191.1(1)/193.3(3)	197.4
C1−E−Al2	118.0	117.4(2)	112.0
C1−E−C6	123.3	122.4(3)	102.2
E−Al2−C13	106.6	109.04(14)	106.2
E−Al2−C15	103.8	105.24(14)	102.8
Al1−E−Al2	139.1		151.3
C11−Al1−C12	121.6	122.7(2)	120.2
N1−Al1−N2	90.1	91.57(14)	97.1

to the experimentally determined values for the complex $Et_2Al(2\text{-}Py)_2N{\rightarrow}AlEt_3$. Because of the coordination of the additional $AlMe_3$ fragment by the bridging nitrogen atom, the $Me_2Al(2\text{-}Py)_2N$ moiety adopts an accentuated butterfly conformation analogous to that of $Me_2Al(2\text{-}Py)_2P$. Furthermore, the heteroatom in the bridging position seems to become a pseudo-sp^3-hybridised centre, giving rise to a displacement of the $AlMe_3$ fragment from the plane containing the N1, E and N2 atoms. Surprisingly, comparison between the model compounds $Me_2Al(2\text{-}Py)_2N{\rightarrow}AlMe_3$ and $Me_2Al(2\text{-}Py)_2P{\rightarrow}AlMe_3$ reveals a different position of the $AlMe_3$ fragment relative to the second aluminium atom of the $Me_2Al(2\text{-}Py)_2E$ butterfly moiety. While both metal atoms are located on the same side in the nitrogen complex, they are positioned on opposite sides in the phosphorus complex (Figure 6).

The experimentally determined Al2→N bond length of 201.0(3) pm in $Et_2Al(2\text{-}Py)_2NAlEt_3$ is significantly longer than a covalent bond and about 5 pm shorter than a pure dative bond.[9] The calculated Al2→N bond length of 212.9 pm in the model complex $Me_2Al(2\text{-}Py)_2N{\rightarrow}AlMe_3$ is much longer, possibly due to the gas-phase nature of the simulation.

The calculated E→Al bond energies at the MP2/6-31+G(d) level for the complexes $Me_3E{\rightarrow}AlMe_3$ (E = N, P) differ from the experimentally determined values only by less than 10 kJ/mol. Consequently, a single-point calculation at the MP2 level of theory was performed for the $Me_2Al(2\text{-}Py)_2N{\rightarrow}AlMe_3$ and $Me_2Al(2\text{-}Py)_2P{\rightarrow}AlMe_3$ complexes. The fully optimised geometry from the BPW91/6−31+G(d) calculations was employed. The calculated bond dissociation energy for the complex $Me_2Al(2\text{-}Py)_2N{\rightarrow}AlMe_3$ (125.4 kJ/mol) is very close to the experimentally determined value for $Me_3N{\rightarrow}AlMe_3$ (129.6 kJ/mol), but the donor-acceptor bond energy of 75.4 kJ/mol in $Me_2Al(2\text{-}Py)_2P{\rightarrow}AlMe_3$ is considerably lower (by 20.7 kJ/mol) than the experimentally determined value for $Me_3P{\rightarrow}AlMe_3$ (96.1 kJ/mol).

In summary, all di(2-pyridyl)amides and -phosphanides coordinate the R_2Al^+ fragment through at least one ring nitrogen atom. This in itself suggests that the charge density in the anions is coupled into the rings and accumulated at the ring nitrogen atoms. The Lewis basicity of the central nitrogen atom in $Me_2Al(2\text{-}Py)_2N$ is still high enough to coordinate a second equivalent of $AlEt_3$ to form the Lewis acid/base adduct $Et_2Al(2\text{-}Py)_2N{\rightarrow}AlEt_3$. All these findings confirm the formation of metal nitrogen rather than of metal−phosphorus bonds even in reaction pathways, as established by Budzelaar for reactions between (2-pyridyl)-phosphanes and methyllithium.[22] The theoretical results presented show that while the bridging nitrogen atom in the amides (E = N) is still a typical Lewis base, the situation in

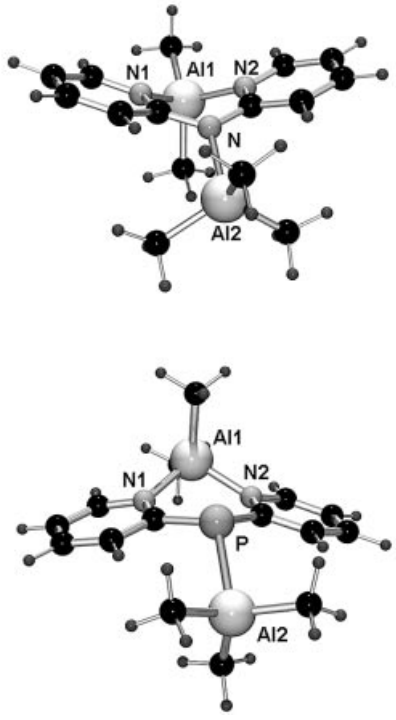

Figure 6. BPW91/6-31+G*-optimised geometries of $Me_2Al(2\text{-}Py)_2N{\rightarrow}AlMe_3$ (top) and $Me_2Al(2\text{-}Py)_2P{\rightarrow}AlMe_3$ (bottom)

the corresponding phosphanides (E = P) is different. Here, nearly all the charge density couples into the pyridyl rings, leaving the central phosphorus atom attractive only for soft metals, in the form of a π-acid-type of coordinating centre to reinforce the otherwise poor phosphorus donor bond energy, shown in the P−N−C allylic coordination to the soft Cs atom.[10c]

Conclusion

The competition between the amidic bridging nitrogen atom and the pyridyl nitrogen atoms for the charge density in Py_2N^- provides for greater conformational variety than in the analogous Py_2E^- systems (E = CH,[7a,7b] P,[10a,10b] As[10b]). The former system shows considerable Lewis basicity at the bridging nitrogen atom, while the charge density at the bridging phosphorus atom is depleted and coupled into the rings. The small energy differences of about 8 kJ/mol between the *cis-trans*, *trans-trans* and *cis-cis* conformers in the Py_2N^- anion can easily be overcome by various crystallisation techniques from different solvents at different temperatures (**1a** from pyridine at 0 °C or from diethyl ether at −40 °C, **1b** from C_6D_6 at room temperature). The 23 kJ/mol by which the *trans-trans* conformer in Py_2P^- is disfavoured against the *cis-trans* form can easily be compensated for by coordination to the hard organometallic Me_2Al^+ fragment. The energy gained from the E→Al donor bonds, in which the charge density at E = N or P can be delocalised to an adjacent carbon atom, is only half the amount with phosphorus than with nitrogen. Hence, the P-centred systems are much better π-donors to soft metals than σ-donors to hard metals. We found computational methods extremely helpful for interpreting the coordination behaviour of di(2-pyridyl)amides and -phosphanides.

Experimental Section

General Remarks: All manipulations were performed under dry N_2 with Schlenk techniques or under argon in a glove box. All solvents were dried with Na/K alloy and distilled prior to use. NMR spectra were obtained in C_6D_6 or $CDCl_3$ as solvent, with $SiMe_4$ or H_3PO_4 as external reference, with a Bruker AMX 250 MHz spectrometer. Mass spectra were recorded with a Finnigan Mat 8230 or Varian Mat CH5 spectrometer. Elemental analyses were performed by the Analytisches Laboratorium, Universität Würzburg.

[Al{(NPy)Py}$_3$] (1a) and/or [Al{(NPy)Py}$_2$(Py$_2$N)] (1b)

1a. Method a: A solution of Py_2NH (4.00 g, 23.3 mmol) in Et_2O (20 mL) was added dropwise to a suspension of $LiAlH_4$ (220 mg, 5.8 mmol) in Et_2O (20 mL), cooled to 0 °C. After the mixture had been stirred at room temp. for 2 d, the diethyl ether was replaced by PyH (20 mL). The reaction mixture was filtered through Celite to remove the undissolved solids, and the clear solution was allowed to stand at 0 °C. After 1 d, crystals of **1a** suitable for single-crystal X-ray diffraction were isolated. For analytic and spectroscopic analysis the crystals were washed twice with hexane (10 mL) and dried under vacuum. Yield: 1.03 g (50%). **Method b:** Py_2NH (2 g, 11.6 mmol) in Et_2O (25 mL) was cooled to −78 °C. Et_3Al (5.95 mL of 15% solution in hexane, 3.83 mmol) was added dropwise to the cooled mixture, which was allowed to gradually attain room temp. Stirring at room temp. was continued for 2 d. Crystals of **1a** suitable for X-ray diffraction study were isolated from the reaction mixture stored at −40°C. For analytical and spectroscopic analysis the crystals were washed twice with hexane (10 mL each time) and dried under vacuum. Yield: 1.85 g (90%). Decomposition point: 83 °C; The ^1H and ^{13}C NMR spectra show different resonance peaks for the coordinated pyridyl ring and noncoordinated pyridyl rings. An unambiguous assignment of all the resonances was not possible. ^1H NMR (C_6D_6): δ = 6.13 (dd, $^3J_{H\text{-}H}$ = 6.2, $^3J_{H\text{-}H}$ = 6.3, 1 H), 6.45 (s_{br}, 1 H,) 7.01 (s_{br}, 2 H, 5-H, 5-H′, 4-H and 4′-H), 7.26 (d, $^3J_{H\text{-}H}$ = 6.6, 1 H,), 7.77 (s_{br}, 1 H), 7.83 (s_{br}, 1 H), 8.12 (s_{br}, 1 H, 3-H, 3′-H, 6-H and 6′-H) ppm. ^{13}C NMR (C_6D_6): δ = 112.0 (s), 113.7 (s), 114.5 (s), 116.3 (s, C-5, C-5′, C-4 and C-4′), 137.5 (s), 138.2 (s), 139.0 (s), 148.1 (s, C-3, C-3′, C-6 and C-6′), 154.1 (s), 160.8 (s, C-2 and C-2′) ppm. EI-MS: *m/z* (%) = 170.1 (100) [Py_2N], 78.1 (24.9) [Py]. $C_{30}H_{24}AlN_9$ (537.56): calcd. C 67.1, H 4.50, N 23.5; found C 65.7, H 4.70, N 23.1.

1b: Compound **1a** was dissolved in C_6D_6 for spectroscopic studies. Reducing the volume of the solution slowly gives rise to crystals of the isomer **1b**. In solution, **1b** converts into **1a**, and hence the spectroscopic data are identical.

[(PyH)$_2$AlCl$_2${(NPy)Py}] (2): A mixture of di(2-pyridyl)amine (0.50 g, 2.90 mmol) and aluminium trichloride (0.39 g, 2.90 mmol) in pyridine (30 mL) was cooled to −40 °C. An equimolar quantity of *n*-butyllithium (1.90 mL of a 1.6 M solution in *n*-hexane) was added dropwise to this mixture, which was gradually allowed to attain room temp. by standing overnight. Stirring of the resulting clear solution at room temp. was continued for 2 d. Needle-shaped, colourless crystals suitable for single-crystal diffraction studies were isolated from the solution after 4 d at 0 °C. After removal of the mother liquor, the crystals were further washed several times with hexane (10 mL) and vacuum-dried for analytic and spectroscopic

studies. Yield: 0.87 g (70.2%). Decomposition point: 50 °C. ^{1}H NMR ($CDCl_3$): δ = 7.04−8.70 (m, 18 H, Py-H) ppm. ^{13}C NMR ($CDCl_3$): δ = 116.6 (s, C-5), 117.7 (s, C-3), 126.6 (s, C_{para}), 139.7 (s, C_{meta}), 141.5 (s, C-4), 142.7 (s, C_{ortho}), 144.1 (s, C-6), 152.8 (s, C-2) ppm. EI-MS: *m*/*z* (%) = 170.1 (12.8) [Py_2N], 119.1 (0.10) [(AlPyN)], 105.1 (0.12) [(AlPy)], 79.1 (100) [PyH]. $C_{20}H_{18}AlCl_2N_5$ (426.28): calcd. C 56.4, H 4.26, N 16.43; found C 54.7, H 4.53, N 15.84.

Crystal Structure Determination: Crystallographic details pertaining to data collection and refinement are presented in Table 7. The data for **1a** and **2** were collected with an Enraf−Nonius CAD4 four-circle diffractometer, and the data for **1b** with a Stoe-IPDS single-circle diffractometer with graphite-monochromated Mo-K_α radiation (λ = 71.073 pm). All data were collected at low temperatures, using oil-coated shock-cooled crystals.[23] After determination and refinement of the cell parameters for **1a** and **2**, the intensity of the reflections was detected by the background-peak-background method.[24] All reflections were collected by the 2θ/ω-scan method for **1a** and **2**, while in the case of **1b** the reflections were detected by the φ-scan mode with stepwise rotation of every 1°. All structures were solved by direct methods by use of the SHELXS-97 program for compounds **1a** and **1b** and SHELXS-96 for **2**.[25a] Refinement of the structures was performed by full-matrix, least-squares methods against F^2 with SHELXL-97[25b] (for **1a** and **1b**) and SHELXL-96[25c] (for **2**). All non-hydrogen atoms were refined with anisotropic displacement parameters. Hydrogen atoms were assigned ideal positions and refined isotropically with a riding model with U_{iso} constrained to 1.2 times of U_{eq} of the parent atom. Structure refinement: Compound **1a** crystallises in the centrosymmetric triclinic space group $P\bar{1}$. The [Al{(NPy)Py}$_3$] (**1a**) molecule shows almost threefold symmetry. In the asymmetric unit, three non-coordinated pyridine molecules are present as solvent from crystallisation. They are not disordered and do not give rise to any hydrogen-bonding pattern. Single-crystal data for compound **1a** in this conformation were obtained in different solvents. Compound **1a** has also been reported by another research group.[13e] The different forms show varying cell parameters, and a comparison of these parameters is listed in the Supporting Information. Compound **1b**, which is a conformational isomer of **1a**, crystallises in the centrosymmetric monoclinic space group $P2_1/c$. Two noncoordinated C_6D_6 solvent molecules are present in the asymmetric unit. The donating pyridine molecules in compound **2** were refined with ADP and distance restraints. Selected bond lengths and angles are summarised in Tables 1−3. The CCDC numbers listed in Table 7 contain the supplementary crystallographic data for this paper. These data can be obtained free of charge at www.ccdc.cam.ac.uk/conts/retrieving.html or from the Cambridge Crystallographic Data Centre, 12, Union Road, Cambridge CB2 1EZ, UK [Fax: (internat.) + 44-1223/336-033; E-mail: deposit@ccdc.cam.ac.uk].

Computational Details: The calculations were carried out with the GAUSSIAN98 program package.[26] For the evaluation of the donor-acceptor bond energies of the complexes $Et_2Al(2\text{-}Py)_2N\rightarrow AlEt_3$ and $Et_2Al(2\text{-}Py)_2P\rightarrow AlEt_3$, calculations at the BPW91,[27] MP2[28] and CBS-4[29] levels of theory were carried out. The 6-31+G(d) basis set was used for the calculations.[30] Because of the

Table 7. Crystallographic data for **1a**, **1b** and **2**

	1a	**1b**	**2**
Empirical formula	$C_{30}H_{24}AlN_9+3C_5H_4N$	$C_{30}H_{24}AlN_9+2C_6D_6$	$C_{20}H_{18}AlCl_2N_5+3C_5H_5N$
CCDC-	180594	180595	180596
Formula mass	774.86	693.78	663.0
Crystal size [mm]	0.2 × 0.3 × 0.5	0.2 × 0.2 × 0.4	0.5 × 0.5 × 0.6
T [K]	173(2)	173(2)	153(2)
Space group	$P\bar{1}$	$P2_1/c$	$P2_1/n$
Crystal system	triclinic	monoclinic	monoclinic
a [pm]	1073.3(3)	969.97(19)	869.4(1)
b [pm]	1387.3(3)	1976.0(4)	2062.5(2)
c [pm]	1425.5(4)	1893.3(4)	1830.3(1)
α [°]	109.556(13)	90	90
β [°]	98.84(2)	105.32(2)	93.723(10)
γ [°]	93.67(2)	90	90
V [nm^3]	1.9612(5)	3.5982(12)	3.2747(4)
Z	2	4	4
ρ_c [Mg m^{-3}]	1.312	1.281	1.346
μ_c [mm^{-1}]	0.103	0.101	0.264
F(000)	812	1456	1384
2θ range [°]	6−50	5−47	6−50
No. of reflns. measd.	7483	14288	11156
No. unique reflns.	6885	4984	4608
No. of restraints	0	0	25
No. of parameters	523	469	415
$R1$[a] [$I > 2\sigma(I)$]	0.043	0.091	0.053
$wR2$[b] (all data)	0.100	0.262	0.101
g_1/g_2 [c]	0.043/0.528	0.157/2.401	0.035/0.543
Largest diff. peak/hole [e·nm^{-3}]	190/−278	1936/−483	502/−252

[a] $R1 = \frac{\sum \left\| F_o \right| - \left| F_c \right\|}{\sum \left| F_o \right|}$ [b] $wR2 = \sqrt{\frac{w(F_o^2 - F_c^2)^2}{w(F_o^2)^2}}$ [c] $w = \frac{1}{\sigma^2(F_o^2) + (g_1 P)^2 + g_2 P}$; $P = \frac{(\max(F_o^2, 0) + 2F_c^2)}{3}$

relatively large size of the bipyridyl complexes, the geometries were fully optimised at the BPW91/6-31+G(d) level and used to compute vibrational harmonic wavenumbers and zero-point corrections. In order to obtain more reliable total energies and bond energies, MP2/6-31+G(d) energy calculations were also performed with the BPW91/6-31+G(d)-optimised geometries, and this type of calculation is designated by the standard notation MP2/6-31+G(d)//BPW91/6-31+G(d).

Acknowledgments

The authors thank the Deutsche Forschungsgemeinschaft (especially the SFB 347, Teilprojekte C2 and D4), the Fonds der Chemischen Industrie and Bruker Nonius, Karlsruhe, for financial support.

[1] J. J. Eisch, in "Aluminium" (Eds.: E. W. Abel, F. G. A. Stone, G. Wilkinson) *Comprehensive Organometallic Chemistry II*, Elsevier, Oxford, UK, **1995**, vol. 1, chapter 10, p. 431 and vol. 11, chapter 6, p. 277.

[2] [2a] D. A. Atwood, *Coord. Chem. Rev.* **1998**, *176*, 407−430. [2b] N. Emig, H. Nguyen, H. Krautscheid, R. Reau, J. B. Cazaux, G. Bertrand, *Organometallics* **1998**, *17*, 3599−3608. [2c] M. Bochmann, D. M. Dawson, *Angew. Chem. Int. Ed. Engl.* **1996**, *35*, 2226−2228; *Angew. Chem.* **1996**, *108*, 2371−2373.

[3] [3a] J. D. Bolt, F. N. Tebbe, *Adv. Ceram.* **1989**, *26*, 69−76. [3b] A. C. Jones, *J. Cryst. Growth* **1993**, *129*, 728−773. [3c] C. Jones, G. A. Koutsantonis, C. L. Raston, *Polyhedron* **1993**, *12*, 1829−1848. [3d] J. Pinkas, T. Wang, R. A. Jacobson, J. G. Verkade, *Inorg. Chem.* **1994**, *33*, 4202−4210. [3e] C. L. Watkins, L. K. Krannich, S. J. Schauer, *Inorg. Chem.* **1995**, *34*, 6228−6230 and references therein. [3f] H. Sussek, O. Stark, A. Devi, H. Pritzkow, R. A. Fischer, *J. Organomet. Chem.* **2000**, *602*, 29−36. [3g] D. C. Bertolet, J. W. Rogers Jr., *Chem. Mater.* **1993**, *5*, 391−395.

[4] [4a] M. F. Lappert, P. P. Power, A. R. Sanger, R. C. Srivastava, *Metal and Metalloid Amides*, E. Horwood, Chichester, **1980**, and references therein. [4b] A. J. Downs, *Chemistry of Aluminium, Gallium, Indium and Thallium*, 1st ed., Blackie, Glasgow, **1993**.

[5] [5a] G. M. Sheldrick, W. S. Sheldrick, *J. Chem. Soc. A* **1969**, 2279−2282. [5b] J. L. Atwood, G. A. Koutsantonis, F. C. Lee, C. L. Raston, *J. Chem. Soc., Chem. Commun.* **1994**, 91−92. [5c] J. T. Leman, J. Braddock-Wilking, A. J. Coolong, A. R. Barron, *Inorg. Chem.* **1993**, *32*, 4324−4336. [5d] J. L. Atwood, S. M. Lawrence, C. L. Raston, *J. Chem. Soc., Chem. Commun.* **1994**, 73−74. [5e] P. Pullmann, K. Hensen, J. W. Bats, *Z. Naturforsch., Teil B* **1982**, *37*, 1312−1315. [5f] P. L. Bellavance, E. R. Corey, J. Y. Corey, G. W. Hey, *Inorg. Chem.* **1977**, *16*, 462−467. [5g] W. Zheng, C. N. Moesch-Zanetti, T. Blunck, H. W. Roesky, M. Noltemeyer, H. -G. Schmidt, *Organometallics* **2001**, *20*, 3299−3303. [5h] N. J. Hardman, C. Cui, H. W. Roesky, W. H. Fink, P. P. Power, *Angew. Chem. Int. Ed.* **2001**, *40*, 2172−2176; *Angew. Chem.* **2001**, *113*, 2230−2232. [5i] C. Cui, H. W. Roesky, H-G. Schmidt, M. Noltemeyer, H. Hao, F. Cimpoesu, *Angew. Chem. Int. Ed.* **2000**, *39*, 4274−4276; *Angew. Chem.* **2000**, *112*, 4444−4446.

[6] T. Kottke, D. Stalke, *Chem. Ber./Recueil* **1997**, *130*, 1365−1374.

[7] [7a] H. Gornitzka, D. Stalke, *Organometallics* **1994**, *13*, 4398−4405. [7b] H. Gornitzka, D. Stalke, *Angew. Chem.* **1994**, *106*, 695−698; *Angew. Chem. Int. Ed. Engl.* **1994**, *33*, 693−695. [7c] U. Pieper, D. Stalke, *Organometallics* **1993**, *12*, 1201−1206. [7d] H. Gornitzka, C. Hemmert, G. Bertrand, M. Pfeiffer, D. Stalke, *Organometallics* **2000**, *19*, 112−114.

[8] H. Gornitzka, D. Stalke, *Eur. J. Inorg. Chem.* **1998**, 311−317.

[9] [9a] M. Pfeiffer, F. Baier, T. Stey, D. Leusser, D. Stalke, B. Engels, D. Moigno, W. Kiefer, *J. Mol. Model.* **2000**, *6*, 299−311. [9b] M. Pfeiffer, F. Baier, T. Stey, D. Leusser, D. Stalke, B. Engels, D. Moigno, W. Kiefer, in *Highlights in Computational Chemistry* (Ed.: T. Clark), Springer-Verlag, Berlin, Heidelberg, **2001**. [9c] L. Mahalakshmi, D. Stalke, in *Structure and Bonding*, vol. 103, 86−115 (Eds.: H. W. Roesky, D. A. Atwood), Springer-Verlag, Berlin, Heidelberg, **2002**.

[10] [10a] A. Steiner, D. Stalke, *J. Chem. Soc., Chem. Commun.* **1993**, 444−446. [10b] A. Steiner, D. Stalke, *Organometallics* **1995**, *14*, 2422−2429. [10c] M. Pfeiffer, T. Stey, H. Jehle, B. Klüpfel, W. Malisch, V. Chandrasekhar, D. Stalke, *Chem. Commun.* **2001**, 337−338.

[11] S. Wingerter, M. Pfeiffer, A. Murso, C. Lustig, T. Stey, V. Chandrasekhar, D. Stalke, *J. Am. Chem. Soc.* **2001**, *123*, 1381−1388.

[12] [12a] S. Wingerter, M. Pfeiffer, F. Baier, T. Stey, D. Stalke, *Z. Anorg. Allg. Chem.* **2000**, *626*, 1121−1130. [12b] S. Wingerter, H. Gornitzka, G. Bertrand, D. Stalke, *Eur. J. Inorg. Chem.* **1999**, *1*, 173−178. [12c] S. Wingerter, H. Gornitzka, R. Bertermann, S. K. Pandey, J. Rocha, D. Stalke, *Organometallics* **2000**, *19*, 3890−3894. [12d] S. Wingerter, M. Pfeiffer, T. Stey, M. Bolboaca, W. Kiefer, V. Chandrasekhar, D. Stalke, *Organometallics* **2001**, *20*, 2730−2735. [12e] A. Steiner, D. Stalke, *Angew. Chem.* **1995**, *107*, 1908−1910; *Angew. Chem. Int. Ed. Engl.* **1995**, *34*, 1752−1755.

[13] [13a] S. Wang, *Coord. Chem. Rev.* **2001**, *215*, 79−98. [13b] J. Ashenhurst, L. Brancaleon, S. Gao, W. Liu, H. Schmider, S. Wang, G. Wu, Q. G. Wu, *Organometallics* **1998**, *17*, 5334−5341. [13c] W. Liu, A. Hassan, S. Wang, *Organometallics* **1997**, *16*, 4257−4259. [13d] X.-M. Wang, H.-S. Sun, X.-Z. You, X. -Y. Huang, *Polyhedron* **1996**, *15*, 3543−3546. [13e] L. M. Engelhardt, M. G. Gardiner, C. Jones, C. P. Junk, L. C. Raston, A. H. White, *J. Chem. Soc., Dalton Trans.* **1996**, 3053−3057.

[14] [14a] A. E. Finholt, A. C. Bond, H. I. Schlesinger, *J. Am. Chem. Soc.* **1947**, *69*, 1199−1203. [14b] E. Wiberg, E. Amberger, *Hydrides of the Elements of the Main Groups 1−4*, Elsevier, Amsterdam, **1971**, p. 285. [14c] G. Liniti, H. Nöth, P. Rahm, *Z. Naturforsch., Teil B* **1988**, *43*, 53−60. [14d] A. Heine, D. Stalke, *Angew. Chem.* **1992**, *104*, 941−942; *Angew. Chem. Int. Ed. Engl.* **1992**, *31*, 854−855. [14e] M. L. Montero, H. Wessel, H. W. Roesky, M. Teichert, I. Usón, *Angew. Chem.* **1997**, *109*, 644−647; *Angew. Chem. Int. Ed. Engl.* **1997**, *36*, 629−631.

[15] [15a] J. E. Johnson, R. A. Jacobson, *Acta Crystallogr., Sect. B* **1973**, *29*, 1669−1674. [15b] G. J. Pyrka, A. A. Pinkerton, *Acta Crystallogr., Sect. C* **1992**, *48*, 91−94. [15c] H. Schödel, C. Näther, H. Bock, F. Butenschön, *Acta Crystallogr. Sect.* **1996**, *52*, 842−853.

[16] P. Rademacher, *Strukturen Organischer Moleküle*, VCH, Weinheim, **1987**.

[17] T. Eicher, S. Hauptmann, *Chemie der Heterocyclen*, VCH, Weinheim, **1995**.

[18] [18a] S. Aduldecha, B. Hathaway, *J. Chem. Soc., Dalton Trans.* **1991**, 993−998. [18b] F. A. Cotton, L. M. Daniels, C. A. Murillo, I. Pascual, *J. Am. Chem. Soc.* **1997**, *119*, 10223−10224.

[19] [19a] A. Haaland, *Angew. Chem.* **1989**, *101*, 1017−1032; *Angew. Chem. Int. Ed. Engl.* **1989**, *28*, 992−1017. [19b] V. Jonas, G. Frenking, M. T. Reetz, *J. Am. Chem. Soc.* **1994**, *116*, 8741−8753.

[20] [20a] A. Almenningen, L. Fernholt, A. Haaland, J. Weidlein, *J. Organomet. Chem.* **1978**, *145*, 109−119. [20b] G. A. Andersen, F. R. Forgaard, A. Haaland, *Acta Chem. Scand.* **1972**, *26*, 1947−1949.

[21] A. E. Reed, R. B. Weinstock, F. Weinhold, *J. Chem. Phys.* **1985**, *82*, 735−746.

[22] [22a] P. H. M. Budzelaar, *J. Org. Chem.* **1998**, *63*, 1131−1137. [22b] G. Talarico, V. Barone, P. H. M. Budzelaar, C. Adamo, *J. Phys. Chem.* **2001**, *105*, 9014−9023.

[23] [23a] D. Stalke, *Chem. Soc. Rev.* **1998**, *27*, 171−178. [23b] T. Kottke, R. J. Lagow, D. Stalke, *J. Appl. Crystallogr.* **1996**, *29*, 465−468. [23c] T. Kottke, D. Stalke, *J. Appl. Crystallogr.* **1993**, *26*, 615−619.

[24] Enraf−Nonius, CAD4 diffractometer program, **1989**.

[25] [25a] G. M. Sheldrick, *Acta Crystallogr., Sect. A* **1990**, *46*,

467−473. [25b] G. M. Sheldrick, *SHELXL-97, Program for crystal structure refinement*, Göttingen **1997**. [25c] G. M. Sheldrick, *SHELXL-96, Program for crystal structure refinement*, Universität Göttingen, **1996**.

[26] M. J. Frisch, G. W. Trucks, H. B. Schlegel, G. E. Scuseria, M. A. Robb, J. R. Cheeseman, V. G. Zakrzewski, J. A. Montgomery, R. E. Stratmann, J. C. Burant, S. Dapprich, J. M. Millam, A. D. Daniels, K. N. Kudin, M. C. Strain, O. Farkas, J. Tomasi, V. Barone, M. Cossi, R. Cammi, B. Mennucci, C. Pomelli, C. Adamo, S. Clifford, J. Ochterski, G. A. Petersson, P. Y. Ayala, Q. Cui, K. Morokuma, D. K. Malick, A. D. Rabuck, K. Raghavachari, J. B. Foresman, J. Cioslowski, J. V. Ortiz, B. B. Stefanov, G. Liu, A. Liashenko, P. Piskorz, I. Komaromi, R. Gomperts, R. L. Martin, D. J. Fox, T. Keith, M. A. Al-Laham, C. Y. Peng, A. Nanayakkara, C. Gonzalez, M. Challacombe, P. M. W. Gill, B. G. Johnson, W. Chen, M. W. Wong, J. L. Andres, M. Head-Gordon, E. S. Replogle, J. A. Pople, *GAUSSIAN98*, Revision A.7, Gaussian, Inc., Pittsburgh, PA, **1998**.

[27] [27a] A. D. Becke, *Phys. Rev.* **1988**, *A38*, 3098−3100. [27b] J. P. Perdew, Y. Wang, *Phys. Rev.* **1992**, *B45*, 13244−13249. [27c] J. P. Perdew, K. Burke, Y. Wang, *Phys. Rev.* **1996**, *B54*, 16533−16539.

[28] C. Møller, M. S. Plesset, *Phys. Rev.* **1934**, *14*, 618−622.

[29] J. W. Ochterski, G. A. Petersson, J. A. Montgomery, *J. Chem. Phys.* **1996**, *104*, 2598−2619.

[30] [30a] R. Ditchfield, W. J. Hehre, J. A. Pople, *J. Chem. Phys.* **1971**, *54*, 724−728. [30b] W. J. Hehre, R. Ditchfield, J. A. Pople, *J. Chem. Phys.* **1972**, *56*, 2257−2261. [30c] P. C. Hariharan, J. A. Pople, *Mol. Phys.* **1974**, *27*, 209−214. [30d] M. S. Gordon, *Chem. Phys. Lett.* **1980**, *76*, 163−168. [30e] P. C. Hariharan, J. A. Pople, *Theor. Chim. Acta* **1973**, *28*, 213−222. [30f] T. Clark, J. Chandrasekhar, G. W. Spitznagel, P. v. R. Schleyer, *J. Comp. Chem.* **1983**, *4*, 294−301.

Received March 5, 2002
[I02115]